

Quantum Simulations of Chemical Reactions: Achieving Accuracy with NISQ Devices

Maitreyee Sarkar,¹ Lisa Roy,¹ Akash Gutal,² Atul Kumar,^{1, a)} and Manikandan Paranjothy^{2, b)}

¹⁾*Quantum Information and Computation Lab, Department of Chemistry, Indian Institute of Technology Jodhpur, Rajasthan, India, 342030*

²⁾*Chemical Dynamics Research Group, Department of Chemistry, Indian Institute of Technology Jodhpur, Rajasthan, India, 342030*

Quantum computing is viewed as a promising technology because of its potential for polynomial growth in complexity, in contrast to the exponential growth observed in its classical counterparts. In the current Noisy Intermediate-Scale Quantum (NISQ) era, the Variational Quantum Eigensolver (VQE), a hybrid variational algorithm, is utilized to simulate molecules using qubits and calculate molecular properties. However, simulating a chemical reaction to compute the reaction energy using VQE algorithm has not yet reached chemical accuracy relative to the benchmark computational chemistry methods due to limitations such as the number of qubits, circuit depth, and noise introduced within the model. To address this issue, we propose the definition of different active spaces for studying chemical reactions, incorporating irreducible representations of both the ground and excited states of the molecules. Our results demonstrate that this approach achieves chemical accuracy in predicting the reaction energy for various reactions. For all reactions studied, the difference in reaction energies between conventional computational chemistry methods and the quantum-classical hybrid VQE algorithm is less than 1 kcal/mol. Furthermore, our analysis simplifies the process of selecting active spaces and electrons for each reaction, reducing it to a single optimal combination that ensures the chemical accuracy for each reaction.

^{a)}Electronic mail: atulk@iitj.ac.in

^{b)}Electronic mail: pmanikandan@iitj.ac.in

I. INTRODUCTION

Quantum mechanics underpins a paradigm shift in computing, redefining the landscape of traditional computing industries. In recent years, quantum computing has transpired as a potential technology characterized by polynomial growth in complexity, in contrast to classical computation, where complexity increases exponentially¹. For example, quantum algorithms like Shor’s algorithm² and Grover’s³ algorithm offer monumental advantages in speed and space over their classical counterparts. These advantages led to applications of quantum algorithms across diverse academic domains within the realms of quantum computing, such as quantum cryptography⁴⁻⁷, quantum key distribution⁷⁻¹⁰, quantum machine learning¹¹⁻¹⁴, quantum finance^{15,16}, and quantum chemistry¹⁷⁻²⁴. Although there are many technological challenges considering the decoherence²⁵⁻²⁸ and scalability of quantum computation, the academic community has witnessed enormous progress on theoretical as well as experimental fronts. With continued advancements in cutting-edge technology, it is possible to envision a quantum computer solving a variety of complex problems efficiently—problems that would be practically intractable with classical computers.

In the past two decades, one of the promising field for the applications of quantum computation has perceived to be computational chemistry. To predict the properties of a molecule, wave function is required and the difficulties in obtaining the wave function increase exponentially with increasing particle numbers^{29,30}. Among modern electronic structure theory methods, the coupled cluster singles, doubles, and perturbative triples, i.e., CCSD(T) method, is expressed to be the gold standard because of its higher accuracy in predicting energies. Compared with the experimental and full Configuration Interaction (CI) data, CCSD(T) produces energy values within a few kJ/mol. However, the scaling of the CCSD(T) method with respect to the size of the system (N) follows $O(N^7)$, limiting its applicability only to a few atom systems. With the advent of quantum computation, quantum computers are becoming essential for understanding molecular properties, as they reduce the problem’s complexity from exponential to the polynomial term.³¹ The unitary coupled cluster (UCC) method is an idea derived from coupled cluster (CC) method of quantum chemistry, as the unitary operations can be naturally executed on a quantum computer.

The theoretical foundation for applying quantum computing to computational chemistry began gaining momentum in the late 1990s³². Zalka demonstrated an efficient simulation of

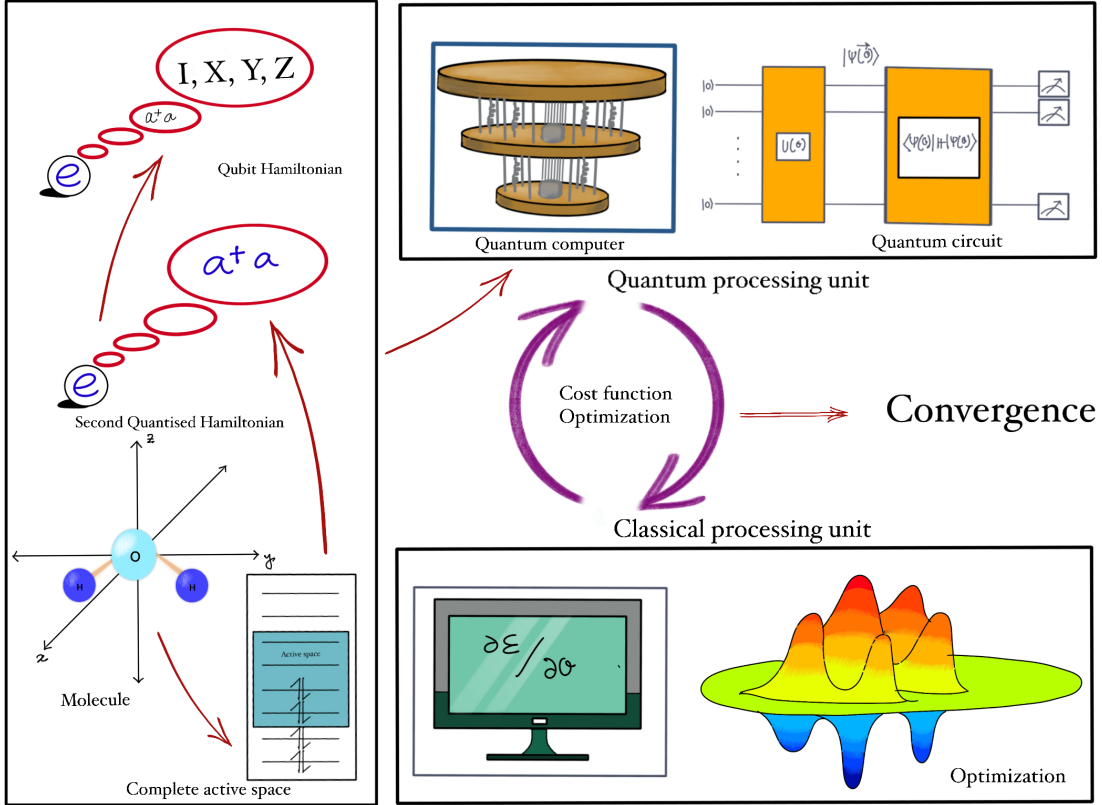


FIG. 1: Schematics of VQE algorithm

the wave function of a many-body system on a quantum computer, with a computational cost comparable to that of conventional classical system simulations³³. One of the best algorithms that can be used for analyzing properties of many-body systems is the quantum phase estimation algorithm (QPEA)³⁴. In comparison to conventional computational techniques available for quantum chemistry calculations, the QPEA shows promises of exponential speedup. However, the main drawback of QPEA is that the circuit depth is very high (i.e., a vast number of quantum gates are required to represent the wavefunction), which is not conceivable without an extensive fault-tolerant quantum computer³⁵.

The quantum computers available today (also called, Near-term quantum devices) are Noisy Intermediate Scale Quantum Computers (NISQ)³⁶ and currently have an insubstantial number of qubits. This motivated the academic community to work with an amalgamated quantum-classical algorithm, i.e., Variational Quantum Eigensolver (VQE)³⁷ for computational chemistry calculations. VQE algorithm has gained significant popularity in near-term quantum devices among the various quantum algorithms used for benchmarking and appli-

cations in computational chemistry, due to its relatively lower circuit depth compared to fault-tolerant quantum computers^{36,38}. In order to compute the ground state energy for any molecule, VQE algorithm utilizes variational principle along with a classical gradient-based optimizer³⁹- a quantum-classical hybrid algorithm. For efficient calculations, a resource conserving approach is to perform the VQE calculations by restricting the Hilbert space, which is defined as active orbitals (which in quantum chemistry is known as active space)⁴⁰. However, due to the limitations in qubit count, circuit depth, and noise in the VQE algorithm, simulating molecular properties does not reach the desired chemical accuracy when compared to traditional computational chemistry methods for various properties of a reaction⁴¹. Here, we efficiently address the question of obtaining the chemical accuracy for a set of reactions using the VQE algorithm and group theory, in comparison to conventional computational chemistry methods.

In this study, we leveraged the point-group symmetry of each reactant and product in a reaction to identify excitations that match the symmetry of ground state energies. Based on these symmetries, we defined the probability of excitations being similar to the ground state. Using the maximum probability among all active spaces for reactants and products, we simulated five different reactions, as shown below, and computed their corresponding reaction energies with the CCSD method and VQE algorithm, achieving the desired chemical accuracy.

- $\text{H}_2 + \text{F}_2 \rightarrow 2 \text{HF}$
- $\text{H}_2 + \text{Cl}_2 \rightarrow 2 \text{HCl}$
- $2 \text{HI} + \text{Cl}_2 \rightarrow 2 \text{HCl} + \text{I}_2$
- $3 \text{H}_2 + \text{CO} \rightarrow \text{CH}_4 + \text{H}_2\text{O}$
- $3 \text{H}_2 + \text{N}_2 \rightarrow 2 \text{NH}_3$

II. BASIC CONCEPTS

A. VQE Algorithm

The fundamental concept behind VQE algorithm is based on the variational principle⁴², which determines an upper bound to actual the ground state energy of a system by using

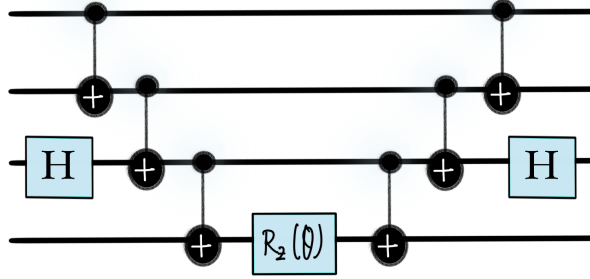


FIG. 2: One term of CCSD ansatz ($Z_1 Z_2 X_3 Z_4$)

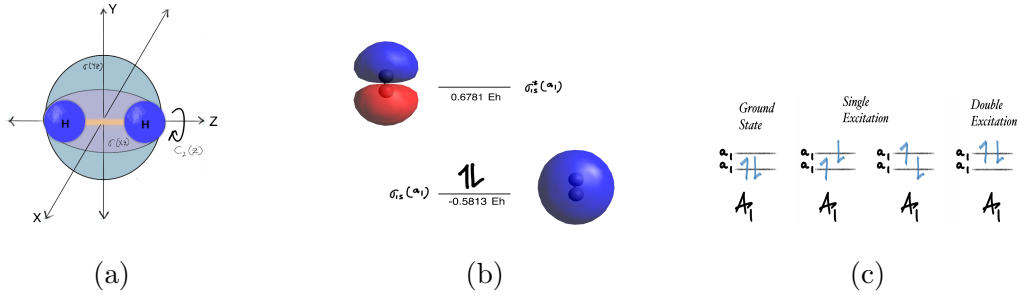


FIG. 3: Different descriptions of H_2 molecule (a)Symmetry operations of H_2 molecule in C_{2v} pointgroup, (b) MO of H_2 molecule and (c)Irreps for excitation of H_2 molecule

a trial wave function that satisfies the problem’s boundary conditions. For instance, if \hat{H} represents the time-independent Hamiltonian and ψ is a suitable trial wave function, then the lowest energy eigenvalue, E_0 , is

$$E_0 \leq \frac{\langle \psi | \hat{H} | \psi \rangle}{\langle \psi | \psi \rangle} \quad (1)$$

In VQE algorithms, the wave function is represented by a parameterized quantum circuit (PQC)^{43–46}, with the aim to variationally optimize⁴⁷ these parameters to minimize the expectation value of the Hamiltonian. As represented in Figure 1, the VQE algorithm consists of several components, each involving key decisions that affect the overall design and cost of the algorithm.

1. Hamiltonian

The transformation of electronic Hamiltonian to a qubit Hamiltonian for optimizing the ground state energy of a molecule using quantum algorithms is a crucial step⁴⁸. For a

molecule containing M nuclei and N electrons, neglecting the relativistic interaction, the molecular Hamiltonian⁴⁹ can be written as

$$\hat{H} = -\sum_{\alpha} \frac{\nabla_{\alpha}^2}{2M_{\alpha}} - \sum_i \frac{\nabla_i^2}{2} - \sum_{\alpha,i} \frac{Z_{\alpha}}{r_{\alpha i}} + \sum_{j>i} \frac{1}{r_{ij}} + \sum_{\beta>\alpha} \frac{Z_{\alpha}Z_{\beta}}{r_{\alpha\beta}} \quad (2)$$

where α and β represent nuclei, M_{α} is the mass of the α -th nuclei, i and j represent electrons, $r_{\alpha i}$ represents the distance between nucleus α and electron i , r_{ij} represents the distance between two electrons i and j , and $r_{\alpha\beta}$ represents the distance between the two nuclei α and β . In Eq. (2), the first two terms correspond to the kinetic energies of the nuclei and electrons, respectively; the third term accounts for the Coulombic attraction between electrons and nuclei; the fourth term represents the Coulombic repulsion between electrons; and the final term describes the Coulombic repulsion between nuclei. As the system size grows with the increasing number of particles, solving the Schrödinger equation becomes increasingly complex and computationally intensive. Given that the nuclei are substantially massive than the electrons, the Born-Oppenheimer approximation⁵⁰ reduces the Hamiltonian by splitting it into nuclear and electronic components, with the electronic Hamiltonian being the focus of quantum chemistry calculations. In general, the electronic Hamiltonian for a molecular system can be expressed as

$$\hat{H}_e = -\sum_i \frac{\nabla_i^2}{2} - \sum_{\alpha,i} \frac{Z_{\alpha}}{r_{\alpha i}} + \sum_{j>i} \frac{1}{r_{ij}} \quad (3)$$

In quantum computation, the purely electronic Hamiltonian is further converted into its second-quantized form by adopting spin-orbital modes, using annihilation and creation operators such that

$$\hat{H}_{SQ} = \sum_{p,q} h_{pq} \hat{a}_p^{\dagger} \hat{a}_q + \frac{1}{2} \sum_{p,q,r,s} h_{pqrs} \hat{a}_p^{\dagger} \hat{a}_q^{\dagger} \hat{a}_r \hat{a}_s \quad (4)$$

where $\hat{a}_i^{\dagger}, \hat{a}_j$ are creation and annihilation operators representing the occupation vector of respective spin orbitals, p, q, r, s denoting the orbital level, and h_{pq} and h_{pqrs} representing one and two electron integrals, respectively.⁵¹ In order to map the quantum chemistry problem to qubits, H_{SQ} can be mapped to a qubit Hamiltonian using Pauli matrices such that the mapping or transformation preserves the necessary commutation relations. Two of the widely used mappings for this transformation are known as Jordan Wigner or the Bravyi-Kitaev transformations⁵¹. The number of qubits required to map H_{SQ} to qubits is equivalent

to the spin orbitals of the molecular system under study. The symmetry consideration in the original system can be further utilized to reduce the dimensionality and complexity of the qubit Hamiltonian. Therefore, a qubit Hamiltonian can be expressed as tensor products of Pauli operators, i.e.,

$$\hat{H}_q = \sum_{\alpha} h_{\alpha} P_{\alpha}; P \in \{I, X, Y, Z\} \quad (5)$$

The transformed Hamiltonian is used to compute the ground state energy of a molecule. It may be noted here that the nuclear-nuclear repulsion energy is calculated and added to the above purely electronic energy to compute the ground state energy and to further compare with the CCSD results.

2. Ansatz

Selecting the appropriate ansatz is a critical aspect of the VQE algorithm. The chosen ansatz should be both sufficiently expressive⁵² and efficiently trainable⁵³ to enable the evaluation of optimized results in a tractable manner. The Unitary Coupled Cluster (UCC) ansatz⁵⁴ is the most dominant approach among several other ansatzes for determining the ground state energy using VQE algorithm. The foundations of UCC lies in Coupled Cluster (CC) theory⁵⁵, which is a post Hartree-Fock method. CC theory improves upon the Hartree-Fock wavefunction by incorporating excitation operators to capture part of the electron correlation energy⁵⁶. The CC singles and doubles (CCSD) excitation theory arises from one and two electron excitations. In general, CC theory includes excitation operators which allow electron transfer from occupied orbitals to virtual orbitals. The coupled-cluster wave function is expressed as

$$|\psi\rangle = e^T |\psi_{\text{HF}}\rangle \quad (6)$$

where $|\psi_{\text{HF}}\rangle$ is the Hartree-Fock wave function. However, the CCSD method is not variational, and the e^T operator is not unitary. To address these limitations, the UCC method leverages the anti-Hermitian property of the operator such that the cluster operator becomes unitary. Therefore, the CC ansatz wave function can be modified to the UCC form as

$$|\psi\rangle = e^{T-T^\dagger} |\psi_0\rangle \quad (7)$$

Since the UCC ansatz needs to be parameterized, it is further expressed using the parameter θ as

$$T = \sum_i \theta_i T_i, \quad (8a)$$

$$T^\dagger = \sum_i \theta_i T_i^\dagger, \quad (8b)$$

To express the exponential as a product of terms, a level-2 trotterization⁴⁷ is applied to the single and double excitations such that

$$U = e^{T-T^\dagger} = \left(\prod_i e^{\frac{\theta_i}{2}(T_i - T_i^\dagger)} \right)^2 \quad (9)$$

In a similar fashion as discussed for the Hamiltonian operator, the operator in Eq. (9) is transformed to Pauli operators using one of the efficient mapping techniques to evolve the unitary operator as

$$U = \left(\prod_i \prod_j e^{i \frac{\theta_i}{2} (P_{ij})} \right)^2 \quad (10)$$

To illustrate how these final qubit terms will be represented in a quantum circuit, the operator term $e^{i \frac{\theta}{2} (Z_1 Z_2 X_3 Z_4)}$ is shown in Figure 2.

3. *Classical optimization*

The third and final component of the VQE algorithm is classical optimization, which is essential to this hybrid quantum-classical approach. Classical optimization algorithms are used to iteratively adjust the parameters of the ansatz until a convergence with expected ground state energy is obtained⁷. For the algorithm to be practically viable, the optimizer must be capable of learning to approximate the solution effectively within a tractable number of steps⁵⁷.

Classical optimization algorithms are divided into gradient-free and gradient-based methods⁷. Gradient-free methods, such as direct search, do not require gradient information of the cost function⁵⁸. In contrast, gradient-based methods involve an optimizer where the gradient (first derivative of the cost function) changes with each iteration. These

methods typically run faster and more smoothly for differentiable functions. For example, Simultaneous Perturbation Stochastic Approximation (SPSA) algorithm is a gradient-based optimization technique that has been successfully implemented to reach ground state energies for small molecules⁵⁷. While the Nelder-Mead simplex algorithm has been used in various experimental studies, gradient-based approaches like the Broyden-Fletcher-Goldfarb-Shanno algorithm (L-BFGS-B), which utilizes limited memory, have outperformed it. Constrained Optimization by Linear Approximations (COBYLA)⁵⁷ is a direct search method known for its robustness to noise and ability to handle constraints, making it useful for VQE algorithm circuits. On the other hand, Sequential Least Squares Quadratic Programming (SLSQP)⁵⁷ is a gradient-based optimizer suitable for both equality and inequality constraints and demonstrates faster convergence compared to gradient-free methods.

B. Group Theory

Group theory⁵⁹⁻⁶² is used to examine the symmetry of a molecule and its impact on various properties of a molecule. By considering the symmetries of the molecular system, it is possible to reduce the dimensions and the complexity of the qubit Hamiltonian⁶³.

III. DETERMINATION OF REACTION ENERGIES USING QUANTUM COMPUTERS

A. Computational Details

1. *Computational Chemistry Methods*

In this article, we utilize NWChem⁶⁴ for the CCSD calculations to optimize and then determine the ground state energies of all the molecules using the frozen-core approximation and STO-3G basis. Additionally, we use Orca⁶⁵ to compute the molecular orbitals for all the molecules with the STO-3G basis set and Avogadro⁶⁶ to visualize the molecular orbitals.

TABLE I: Character table⁷⁰ for C_{2v} point group

C_{2v}	E	$C_2(z)$	$\sigma_v(xz)$	$\sigma_v(yz)$
A_1	1	1	1	1
A_2	1	1	-1	-1
B_1	1	-1	1	-1
B_2	1	-1	-1	1

TABLE II: Product table⁷⁰ for C_{2v} point group

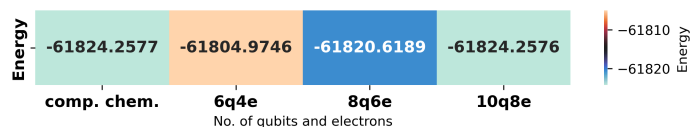
	A_1	A_2	B_1	B_2
A_1	A_1	A_2	B_1	B_2
A_2	A_2	A_1	B_2	B_1
B_1	B_1	B_2	A_1	A_2
B_2	B_2	B_1	A_2	A_1

2. Quantum Computation Methods

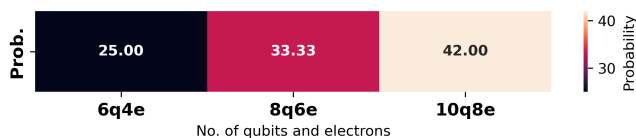
To compute the reaction energy using a quantum computer, we utilize Qiskit 0.46.0⁶⁷, Qiskit Nature 0.6.0⁶⁸, and PySCF 2.0.1⁶⁹. The ground state energies are calculated using the STO-3G basis set, UCCSD ansatz, and the statevector simulator.

B. Mathematical details of Group theory

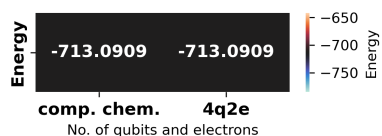
Figure 3(a) shows the symmetry operations of the C_{2v} point group for the H_2 molecule. Additionally, we analyze the direct products of the irreducible representations (irreps) using the product table for the C_{2v} irreps, which is presented in Table II. For instance, Fig. 3(b) illustrates that two $1S$ atomic orbitals (AOs) from each hydrogen atom combine to form molecular orbitals (MOs) for the hydrogen molecule, both having the irrep a_1 . Figure 3(c) illustrates the irreps of the ground and excited states for a molecule, using the hydrogen molecule as an example. Since the H_2 molecule belongs to the $D_{\infty h}$ point group, we select the abelian subgroup C_{2v} (shown in Table I) for simplicity in calculations.



(a) Energy values for HF Molecule



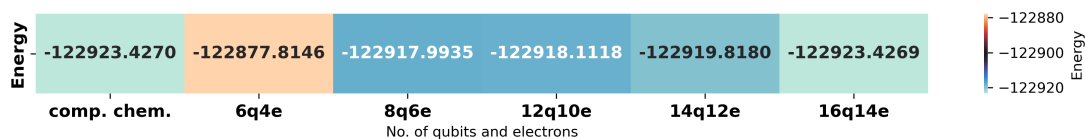
(b) Probability values for HF Molecule



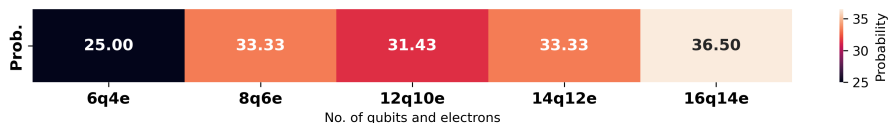
(c) Energy values for H₂ molecule



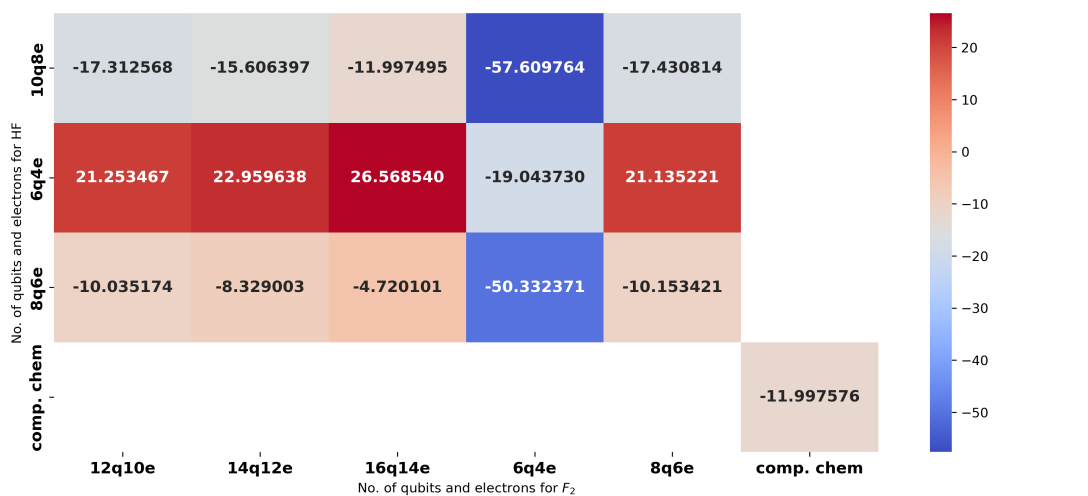
(d) Probability values for H₂ molecule



(e) Energy values for F₂ molecule



(f) Probability values for F₂ molecule



(g) Combinations of reaction energies for the generation of HF from H₂ and F₂

FIG. 4: Energy and probability values for reactants, products and reaction energies of

Reaction 1.

As a result, the ground state of the H_2 molecule corresponds to the irrep $a_1 \times a_1 = A_1$. Furthermore, as shown in Figure 3(c), for the H_2 molecule, two single excitations and one double excitation are possible, and all excitation terms possess the A_1 irrep (see Table II). Consequently, all excitation terms share the same irrep as the ground state of the H_2 molecule.

C. Results

1. $\text{H}_2 + \text{F}_2 \rightarrow 2 \text{HF}$

We now proceed to perform a comprehensive analysis of a set of closed-shell chemical reactions to estimate reaction energies using computational chemistry and the VQE algorithm. To begin with, we consider fluorination of hydrogen which is an exothermic reaction. We evaluate the single-point energy for the previously optimized geometries of all the reactants and products using NWChem. As illustrated in Figures 4(a-f), we employ various combinations of spin-orbitals (qubits) and electrons for the VQE algorithm calculations. The reaction energy obtained using the CCSD method is used as the reference to estimate the accuracy of the VQE algorithm calculations. Our analysis using VQE algorithm demonstrates that based on spin orbitals and number of electrons, there are a total of 15 combinations required to be optimally analyze and evaluate the reaction energy. Figure 4(g) shows that not all of the 15 possible combinations achieve chemical accuracy.

To visualize this result, let us first briefly analyze the active space for the HF molecule. For example, Figure 6 shows three different active spaces (6-qubit, 4-electron; 8-qubit, 6-electron; 10-qubit, 8-electron) for the HF molecule. The active space includes a maximum of five MOs and eight electrons. The energy of the sixth MO ($-25.907079 E_h$) is much lower than that of the fifth and fourth MOs ($-1.450018 E_h$ and $-0.561731 E_h$, respectively), as seen in Figure 5. Therefore, the sixth MO has not been considered for the VQE algorithm calculations. The first active space includes six qubits and four electrons due to the two degenerate MOs in the HOMO, and hence the first active space will include three MOs instead of two, as represented in Figures 5 and 4(a). Based on the molecular orbitals, the **minimum number** of qubits required for H_2 , F_2 , and HF are 4, 6, and 6, respectively. The orbital energies for the F_2 molecule are provided in the supporting information. We

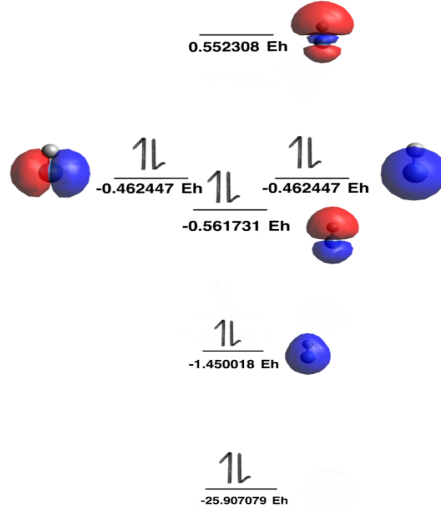
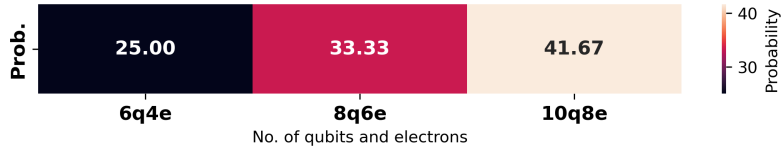
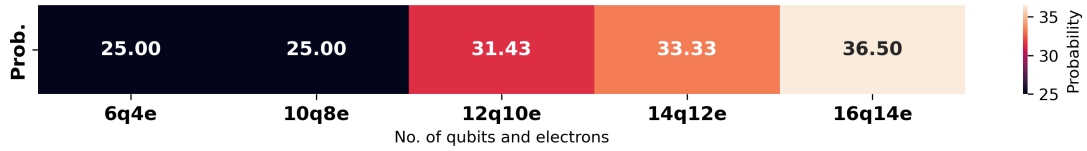


FIG. 5: MO of HF molecule (image is not upto scale)



(a) Probability values for HCl Molecule



(b) Probability values for Cl₂ molecule

FIG. 6: Probability values for reactants and products of Reaction 2.

further analyze the irreducible representations for all combinations of MOs and electrons for reactants and products for each single and double excitation term to determine how many transitions have the same irreducible representation as the ground state.

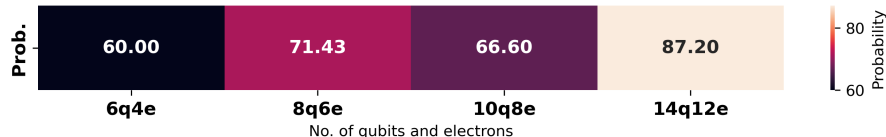
The HF molecule is a linear diatomic molecule with the point group symmetry $D_{\infty h}$, a non-abelian group. To simplify the calculations, we use the abelian subgroup C_{2v} to determine the irreducible representations of the molecular orbitals and molecular excitations. We find that the irreducible representation for the ground state is A_1 . Similarly, four of the single excitations and four of the double excitations, out of the total eight excitations, correspond to the irreps B_2 , B_2 , A_2 , A_2 and A_1 , A_1 , B_1 , B_1 , respectively. This indicates

that 25% of the excitations share the same irreps as the ground state, as seen in Figure 4(b). Similarly, we calculate the irreducible representations for all the active spaces of reactants and products, and determine how many of them match the ground state. Based on these numbers, we define the probability. For example, if all the excitations share the same irreducible representation as the ground state, we assign a probability of 100%, and if only half of the excitations match the symmetry of ground state, then the probability is 50%.

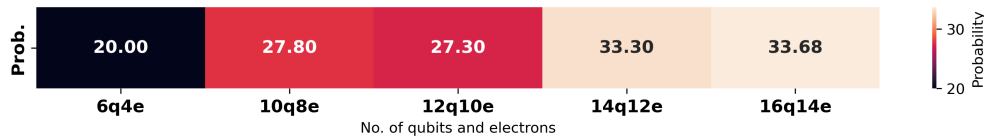
As shown in Figure 4(e), for the F_2 molecule, the largest active space considered in our calculations is a 16-qubit, 14-electron system. For our purpose, two core molecular orbitals were excluded from the calculation because the energy gap between the MOs considered for calculation and the two core MOs is very large, which would significantly increase the computational cost in VQE algorithm. Figure 4(d) shows that for the H_2 molecule, the 4-qubit, 2-electron method has the symmetry of all excitation terms matching the ground state, resulting in a probability of 100%. In contrast, Figures 4(b) and 4(f) show that for HF (the 10-qubit, 8-electron case) and F_2 (the 16-qubit, 14-electron case), the maximum probabilities are 42% and 36.5%, respectively. Clearly, Figure 4(g) demonstrates that the combination of maximum probabilities for all cases achieves chemical accuracy when compared to our CCSD calculations with an accuracy of the order 10^{-5} , as can be seen in Figure 11, which holds the same comparison for all five reactions.

2. $H_2 + Cl_2 \rightarrow 2 HCl$

The next reaction studied is the exothermic chlorination of hydrogen. As shown in Figure 6(a), for the HCl molecule, the largest active space used in our calculation is a 10-qubit, 8-electron system. Similarly, for the Cl_2 molecule, as depicted in Figure 6(b), the largest active space is a 16-qubit, 14-electron system. Figures 6(a) and 6(b) also highlight that, for both HCl and Cl_2 , these active spaces correspond to the maximum probabilities— 41.67% and 36.5%, respectively. Clearly, Figure 10, which displays the energy values calculated for all the studied reactions, demonstrates that the combination of maximum probabilities achieves chemical accuracy, with an accuracy on the order of 10^{-4} , out of all 15 possible combinations, as shown in Figure 11. The respective energy values for the different active spaces are available in the supporting information.



(a) Probability values for HI Molecule



(b) Probability values for I₂ molecule

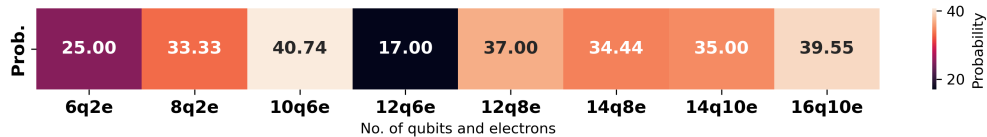
FIG. 7: Probability values for reactants and products of Reaction 3.

3. $2 \text{HI} + \text{Cl}_2 \rightarrow 2 \text{HCl} + \text{I}_2$

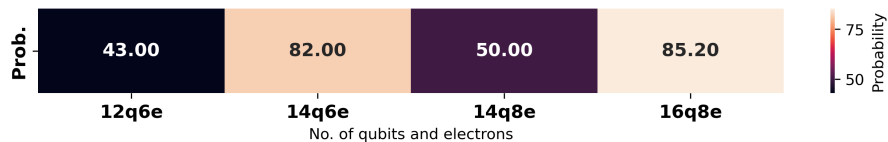
The third reaction considered is the halogen displacement reaction of chlorine and iodine. As shown in Figure 7(a), for the HI molecule, the largest active space is a 14-qubit, 12-electron system. Similarly, for the I₂ molecule, as illustrated in Figure 7(b), the largest active space is a 16-qubit, 14-electron system. Figures 7(a) and 7(b) also reveal that, for both HI and I₂, these largest active spaces correspond to the maximum probabilities - 87.2% and 33.68%, respectively. Figure 10 demonstrates that the combination of maximum probabilities achieves chemical accuracy, with an error on the order of 10^{-1} , out of all 300 possible combinations, as shown in Figure 11. The respective energy values for the different active spaces can be found in the supporting information.

4. $3 \text{H}_2 + \text{CO} \rightarrow \text{CH}_4 + \text{H}_2\text{O}$

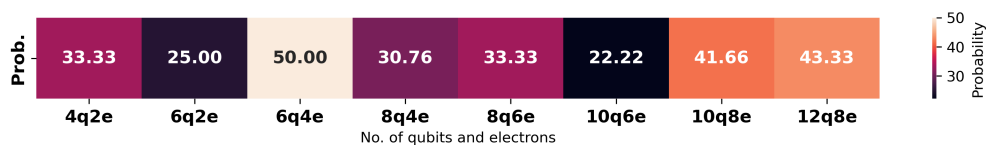
The fourth reaction studied is the hydrogenation of carbon monoxide, which is known as the Sabatier reaction for the generation of methane from carbon monoxide. Figure 8(a) shows that for the CO molecule, the 16-qubit, 10-electron active space is the largest system considered for the purpose of calculation in this article. Similarly, figures 8(b) and 8(c) show that the largest active space for CH₄ and H₂O molecules are 16-qubit, 8-electron and 12-qubit, 8-electron systems, respectively. Figures 8(a), 8(b), and 8(c) further demonstrate that for CO, CH₄, and H₂O, 10-qubit 6-electron, 16-qubit 8-electron, and 6-qubit 4-electron systems, lead to the maximum probabilities of 40.74%, 85.2% and 50%, respectively. Figure



(a) Probability values for CO Molecule

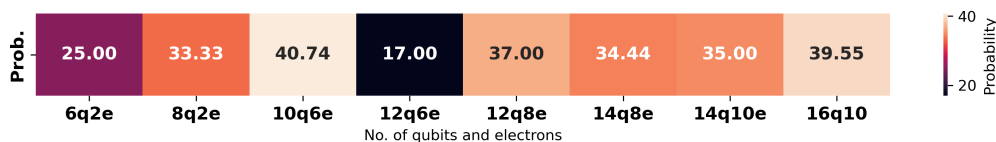


(b) Probability values for CH₄ molecule

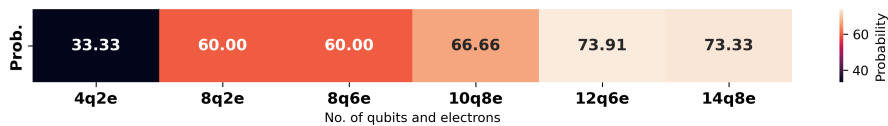


(c) Probability values for H₂O molecule

FIG. 8: Probability values for reactants and products of Reaction 4.



(a) Probability values for N₂ Molecule



(b) Probability values for NH₃ molecule

FIG. 9: Probability values for reactants and products of Reaction 5.

10 demonstrates that the combination of maximum probabilities achieves chemical accuracy with an accuracy of the order of 10^{-3} out of all possible 256 combinations as shown in Figure 11. Respective energy values for different active spaces are available in the supporting information.

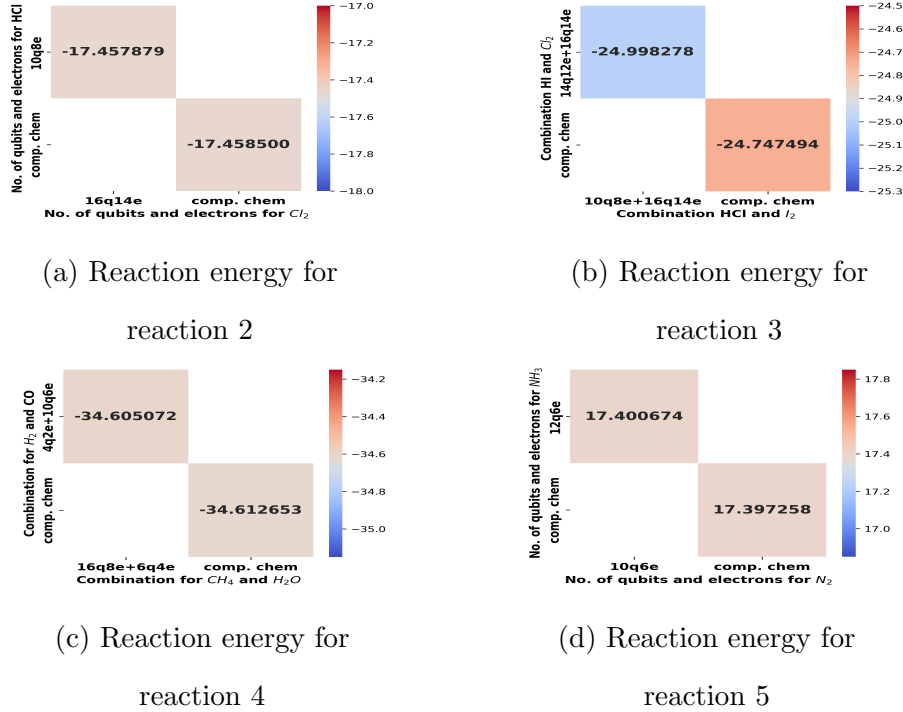


FIG. 10: All reaction energies considering the best combinations

5. $3\text{H}_2 + \text{N}_2 \rightarrow 2\text{NH}_3$

The final reaction considered is the synthesis of ammonia, which is a crucial step in the Haber process for synthesising ammonia for fertilisers (nitrogen fixation). As shown in Figure 9(a), for the N_2 molecule, the largest active space is a 16-qubit, 10-electron system. Similarly, for the NH_3 molecule, as depicted in Figure 9(b), the largest active space is a 14-qubit, 8-electron system. Figures 9(a) and 9(b) also indicate that for N_2 and NH_3 , the 10-qubit, 6-electron, and 12-qubit, 6-electron systems, the maximum probabilities are 40.74% and 73.91%, respectively. Figure 10 demonstrates that the combination of these maximum probabilities achieves chemical accuracy with error of the order of 10^{-3} , out of all 48 possible combinations, as shown in Figure 11. The respective energy values for the different active spaces are available in the supporting information.

D. Analysis

The significance of the findings in the present work in addressing computational chemistry problems in the realm of quantum computation, particularly within the limitations of the

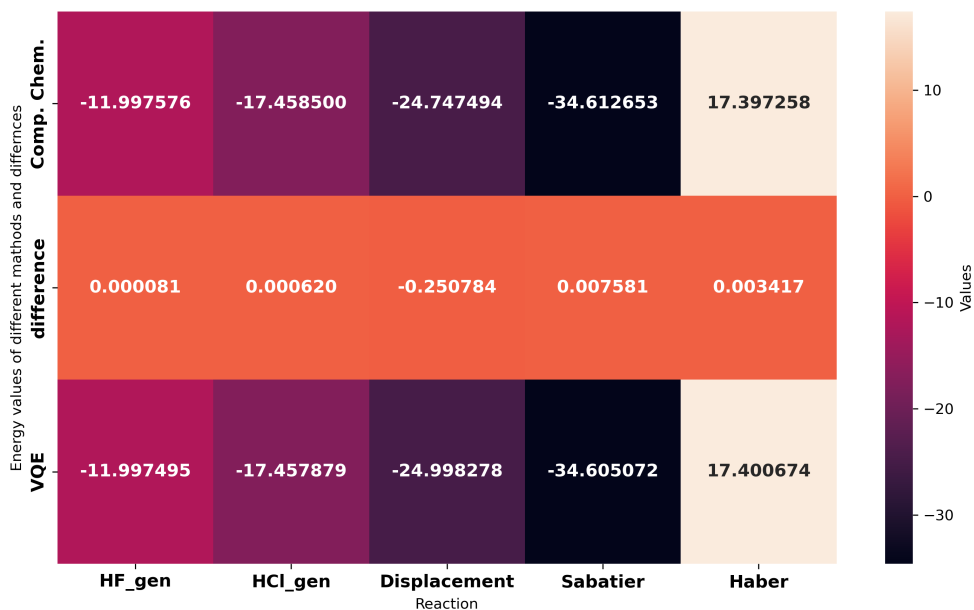


FIG. 11: Comparison of energy values for all five reactions

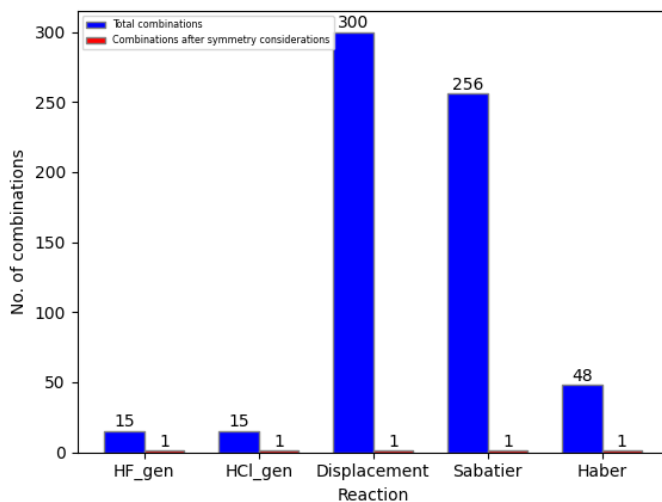


FIG. 12: Reduction in the number of combinations

NISQ era, can be summarized as follows:

a. Validation of chemical accuracy We validated the defined scheme for five different reactions, generating expected results for all cases. For all five reactions, the difference in reaction energies between conventional computational chemistry methods and the quantum-classical hybrid VQE algorithm is less than 1 kcal/mol, signifying chemical accuracy, as shown in Figure 11.

b. Effect of increased active space As the active space increases, the ground state energy evaluated using our approach converges to the CCSD value.

c. Reduction in the number of combinations Our analysis has successfully reduced the number of combinations for each reaction to just a single combination. For instance, out of 15 combinations for the first two reactions, 300 combinations for the third reaction, 256 combinations, and 48 combinations for the last reaction, only one combination is needed for each case, as seen in Figure 12.

d. Dependence on molecular size For reactions where most of the molecular orbitals were considered as part of the active space in the calculations (e.g., reactions 1, 2, 4, and 5), the reaction energy difference between the CCSD method and VQE algorithm energies is accurate to or less than two decimal points, as shown in Figure 11. However, for the larger molecule in reaction 3 (involving I_2 and HI), when a large portion of the molecular orbitals (MOs) remains uninvolved in the active space, the difference in reaction energy is a bit higher. Nevertheless, it still remains within the limit of chemical accuracy, as can be observed in Figures 10(b) and 11.

IV. CONCLUSION

Variational algorithms have emerged as a key approach in utilizing NISQ devices for complex optimization problems, operating within a hybrid quantum-classical framework. However, despite their promising potential on NISQ devices, their performance has not met expectations due to several challenges, including noise-sensitive quantum gates, limited qubit connectivity, and the issue of barren plateaus. Therefore, simulating molecules on a quantum computer presents a different set of challenges in the NISQ era, particularly when considering various active spaces for ground state energy (GSE) calculations. As the active spaces increase, the complexity of the calculations also increases. Due to the limited power of NISQ devices, computations involving more than 16 qubits become computationally expensive.

To overcome some of these challenges, we have developed a scheme to construct the optimal combination of qubits (from the molecular orbitals) and electrons for different products and reactants. This is achieved by utilizing their respective irreducible representations of the ground state and all excited states, which allows us to reach chemical accuracy compared

to traditional computational chemistry methods. We tested the scheme on five different reactions and observed consistent results across all cases. The scheme successfully reduces the number of combinations to just one out of all possible combinations for each reaction. As shown in Figure 11, for all five reactions, the energy difference is less than 1 kcal/mol. Furthermore, this scheme has reduced the number of combinations for each reaction to a single combination, down from 15 combinations for the first two reactions, 300 combinations for the third reaction, 256 combinations for the fourth reaction, and 48 combinations for the last reaction, as illustrated in Figure 12. The reaction energies calculated using this method for reactions with smaller reactants and products show CCSD method and VQE algorithm energies that are accurate to or less than two decimal points. For larger molecules, the energy difference is higher but still remains within the limit of chemical accuracy, as shown in Figures 10(b) and 11.

As part of our future work, we will investigate how this scheme performs with larger basis sets and whether chemical accuracy can still be achieved in such scenarios, as the molecular orbitals become significantly more complex. Additionally, we plan to explore the use of symmetry methods to simplify the Hamiltonian and wave functions in order to simulate different reactions and reduce computational costs. We will also examine the impact of noise on the results and explore error mitigation techniques that leverage symmetry relations to achieve chemical accuracy in quantum chemistry problems.

ACKNOWLEDGMENTS

MS, LR, APG, AK, and PM gratefully acknowledge the Indian Institute of Technology, Jodhpur, for providing the computational facilities essential for completing this work. AK also acknowledges SERB (Grant No. CRG/2022/005979) for funding the project. MS further thanks the Department of Chemistry, IIT Jodhpur, and the Ministry of Education (MoE) for offering research infrastructure and financial support. The authors also extend their appreciation to IBM for providing access to IBM Quantum Systems.

REFERENCES

- ¹E. Rieffel and W. Polak, “An introduction to quantum computing for non-physicists,” *ACM Comput. Surv.* **32**, 300–335 (2000).
- ²P. W. Shor, “Polynomial-time algorithms for prime factorization and discrete logarithms on a quantum computer,” *SIAM Rev.* **41**, 303–332 (1999).
- ³L. K. Grover, “A fast quantum mechanical algorithm for database search,” in *Proceedings of the twenty-eighth annual ACM symposium on Theory of computing* (1996) pp. 212–219.
- ⁴S. Pirandola, U. L. Andersen, L. Banchi, M. Berta, D. Bunandar, R. Colbeck, D. Englund, T. Gehring, C. Lupo, C. Ottaviani, *et al.*, “Advances in quantum cryptography,” *Adv. Opt. Photonics* **12**, 1012–1236 (2020).
- ⁵C. H. Bennett, G. Brassard, and A. K. Ekert, “Quantum cryptography,” *Sci. Am.* **267**, 50–57 (1992).
- ⁶C. H. Bennett, F. Bessette, G. Brassard, L. Salvail, and J. Smolin, “Experimental quantum cryptography,” *J. Cryptol.* **5**, 3–28 (1992).
- ⁷M. A. Nielsen and I. L. Chuang, “Quantum computation and quantum information,” *Phys. Today* **54**, 60 (2001).
- ⁸P. W. Shor and J. Preskill, “Simple proof of security of the bb84 quantum key distribution protocol,” *Phys. Rev. Lett.* **85**, 441 (2000).
- ⁹R. Renner, “Security of quantum key distribution,” *Int. J. Quantum Inf.* **6**, 1–127 (2008).
- ¹⁰R. Wolf, “Quantum key distribution,” *Lect. Notes Phys.* **988** (2021).
- ¹¹M. Schuld, I. Sinayskiy, and F. Petruccione, “An introduction to quantum machine learning,” *Contemp. Phys.* **56**, 172–185 (2015).
- ¹²C. Ciliberto, M. Herbster, A. D. Ialongo, M. Pontil, A. Rocchetto, S. Severini, and L. Wossnig, “Quantum machine learning: a classical perspective,” *Proc. R. Soc. A: Math. Phys. Eng. Sci.* **474**, 20170551 (2018).
- ¹³H.-Y. Huang, M. Broughton, M. Mohseni, R. Babbush, S. Boixo, H. Neven, and J. R. McClean, “Power of data in quantum machine learning,” *Nat. Commun.* **12**, 2631 (2021).
- ¹⁴D. Sharma, P. Singh, and A. Kumar, “Quantum-inspired attribute selection algorithms,” *Quantum Sci. Technol.* **10**, 015036 (2024).
- ¹⁵R. Orús, S. Múgel, and E. Lizaso, “Quantum computing for finance: Overview and prospects,” *Rev. Phys.* **4**, 100028 (2019).

- ¹⁶Y.-J. Chang, M.-F. Sie, S.-W. Liao, and C.-R. Chang, “The prospects of quantum computing for quantitative finance and beyond,” *IEEE Nanotechnol. Mag.* **17**, 31–37 (2023).
- ¹⁷Y. Cao, J. Romero, J. P. Olson, M. Degroote, P. D. Johnson, M. Kieferová, I. D. Kivlichan, T. Menke, B. Peropadre, N. P. Sawaya, *et al.*, “Quantum chemistry in the age of quantum computing,” *Chem. Rev.* **119**, 10856–10915 (2019).
- ¹⁸S. McArdle, S. Endo, A. Aspuru-Guzik, S. C. Benjamin, and X. Yuan, “Quantum computational chemistry,” *Rev. Mod. Phys.* **92**, 015003 (2020).
- ¹⁹B. P. Lanyon, J. D. Whitfield, G. G. Gillett, M. E. Goggin, M. P. Almeida, I. Kassal, J. D. Biamonte, M. Mohseni, B. J. Powell, M. Barbieri, *et al.*, “Towards quantum chemistry on a quantum computer,” *Nat. Chem.* **2**, 106–111 (2010).
- ²⁰D. Claudino, “The basics of quantum computing for chemists,” *Int. J. Quantum Chem.* **122**, e26990 (2022).
- ²¹S. Kais, “Introduction to quantum information and computation for chemistry,” *Quantum Inf. Comp. Chem.* , 1–38 (2014).
- ²²G. Fano and S. Blinder, “Quantum chemistry on a quantum computer,” in *Mathematical Physics in Theoretical Chemistry* (Elsevier, 2019) pp. 377–400.
- ²³I. Kassal, J. D. Whitfield, A. Perdomo-Ortiz, M.-H. Yung, and A. Aspuru-Guzik, “Chapter 11—simulating chemistry using quantum computers,” *Annu. Rev. Phys. Chem.* **62**, 185–207 (2011).
- ²⁴P. A. M. Dirac, “Quantum mechanics of many-electron systems,” *Proc. R. Soc. Lond. A.* **123**, 714–733 (1929).
- ²⁵H. E. Brandt, “Qubit devices and the issue of quantum decoherence,” *Prog. Quantum Electron.* **22**, 257–370 (1999).
- ²⁶J. P. Barnes and W. S. Warren, “Decoherence and programmable quantum computation,” *Phy. Rev. A.* **60**, 4363 (1999).
- ²⁷D. DiVincenzo and B. Terhal, “Decoherence: the obstacle to quantum computation,” *Phys. World* **11**, 53 (1998).
- ²⁸V. B. Sabale, N. R. Dash, A. Kumar, and S. Banerjee, “Facets of correlated non-markovian channels,” *Ann. Phys. (Berlin)* **536**, 2400151 (2024).
- ²⁹A. Aspuru-Guzik, A. D. Dutoi, P. J. Love, and M. Head-Gordon, “Simulated quantum computation of molecular energies,” *Science* **309**, 1704–1707 (2005).
- ³⁰V. Armaos, D. A. Badounas, P. Deligiannis, and K. Lianos, “Computational chemistry

- on quantum computers: Ground state estimation,” *Appl. Phys. A.* **126**, 625 (2020).
- ³¹R. P. Feynman, “Simulating physics with computers,” *Int. J. Theor. Phys.* **21**, 467–488 (1982).
- ³²C. Zalka, “Efficient simulation of quantum systems by quantum computers,” *Fortschr. Phys.* **46**, 877–879 (1998).
- ³³G. Ortiz, J. E. Gubernatis, E. Knill, and R. Laflamme, “Quantum algorithms for fermionic simulations,” *Phys. Rev. A.* **64**, 022319 (2001).
- ³⁴M. Motta and J. E. Rice, “Emerging quantum computing algorithms for quantum chemistry,” *Wiley Interdiscip. Rev. Comput. Mol. Sci.* **12**, e1580 (2022).
- ³⁵J. B. Parker and I. Joseph, “Quantum phase estimation for a class of generalized eigenvalue problems,” *Phys. Rev. A* **102**, 022422 (2020).
- ³⁶J. Preskill, “Quantum computing in the nisq era and beyond,” *Quantum* **2**, 79 (2018).
- ³⁷A. Kandala, A. Mezzacapo, K. Temme, M. Takita, M. Brink, J. M. Chow, and J. M. Gambetta, “Hardware-efficient variational quantum eigensolver for small molecules and quantum magnets,” *Nature* **549**, 242–246 (2017).
- ³⁸Y. Li, J. Hu, X.-M. Zhang, Z. Song, and M.-H. Yung, “Variational quantum simulation for quantum chemistry,” *Adv. Theory Simul.* **2**, 1800182 (2019).
- ³⁹A. Peruzzo, J. McClean, P. Shadbolt, M.-H. Yung, X.-Q. Zhou, P. J. Love, A. Aspuru-Guzik, and J. L. O’Brien, “A variational eigenvalue solver on a photonic quantum processor,” *Nat. Commun.* **5**, 4213 (2014).
- ⁴⁰S. Yalouz, B. Senjean, J. Günther, F. Buda, T. E. O’Brien, and L. Visscher, “A state-averaged orbital-optimized hybrid quantum–classical algorithm for a democratic description of ground and excited states,” *Quantum Sci. Technol.* **6**, 024004 (2021).
- ⁴¹I. Liepuoniute, M. Motta, T. Pellegrini, J. E. Rice, T. P. Gujarati, S. Gil, and G. O. Jones, “Simulation of a diels-alder reaction on a quantum computer,” arXiv preprint arXiv:2403.08107 (2024).
- ⁴²D. A. McQuarrie and J. D. Simon, *Physical chemistry: a molecular approach*, Vol. 1 (University science books Sausalito, CA, 1997).
- ⁴³M. Ostaszewski, E. Grant, and M. Benedetti, “Structure optimization for parameterized quantum circuits,” *Quantum* **5**, 391 (2021).
- ⁴⁴M. Benedetti, E. Lloyd, S. Sack, and M. Fiorentini, “Parameterized quantum circuits as machine learning models,” *Quantum Sci. Technol.* **4**, 043001 (2019).

- ⁴⁵J. D. Whitfield, J. Biamonte, and A. Aspuru-Guzik, “Simulation of electronic structure hamiltonians using quantum computers,” *Mol. Phys.* **109**, 735–750 (2011).
- ⁴⁶J. Lee, W. J. Huggins, M. Head-Gordon, and K. B. Whaley, “Generalized unitary coupled cluster wave functions for quantum computation,” *J. Chem. Theory Comput.* **15**, 311–324 (2018).
- ⁴⁷J. Romero, R. Babbush, J. R. McClean, C. Hempel, P. J. Love, and A. Aspuru-Guzik, “Strategies for quantum computing molecular energies using the unitary coupled cluster ansatz,” *Quantum Sci. Technol.* **4**, 014008 (2018).
- ⁴⁸M. Alteg, B. Chevalier, O. Mestoudjian, and J.-L. Rossi, “Study of adaptative derivative-assemble pseudo-trotter ansatzes in vqe through qiskit api,” arXiv preprint arXiv:2210.15438 (2022).
- ⁴⁹P. Carsky and M. Urban, *Ab initio calculations: methods and applications in chemistry*, Vol. 16 (Springer Science & Business Media, 2012).
- ⁵⁰M. Born and J. Oppenheimer, “Zur quantentheorie der molekeln,” *Ann. Phys.* **84**, 457–484 (1927).
- ⁵¹D. A. Fedorov, B. Peng, N. Govind, and Y. Alexeev, “Vqe method: a short survey and recent developments,” *Mater. Theory* **6**, 2 (2022).
- ⁵²S. Sim, P. D. Johnson, and A. Aspuru-Guzik, “Expressibility and entangling capability of parameterized quantum circuits for hybrid quantum-classical algorithms,” *Adv. Quantum Technol.* **2**, 1900070 (2019).
- ⁵³A. Skolik, *Quantum machine learning: On the design, trainability and noise-robustness of near-term algorithms*, Ph.D. thesis, Leiden University (2023).
- ⁵⁴H. R. Grimsley, D. Claudino, S. E. Economou, E. Barnes, and N. J. Mayhall, “Is the trotterized uccsd ansatz chemically well-defined?” *J. Chem. Theory Comput.* **16**, 1–6 (2019).
- ⁵⁵R. J. Bartlett, *Coupled-cluster theory: An overview of recent developments* (World Scientific, 1995) pp. 1047–1131.
- ⁵⁶Y. Shikano, H. C. Watanabe, K. M. Nakanishi, and Y.-y. Ohnishi, “Post-hartree-fock method in quantum chemistry for quantum computer,” *Eur. Phys. J. Spec. Top.* **230**, 1037–1051 (2021).
- ⁵⁷H. Singh, S. Majumder, and S. Mishra, “Benchmarking of different optimizers in the variational quantum algorithms for applications in quantum chemistry,” *J. Chem. Phys.* **159** (2023).

- ⁵⁸W. Lavrijsen, A. Tudor, J. Müller, C. Iancu, and W. De Jong, “Classical optimizers for noisy intermediate-scale quantum devices,” in *2020 IEEE international conference on quantum computing and engineering (QCE)* (IEEE, 2020) pp. 267–277.
- ⁵⁹F. A. Cotton, *Chemical applications of group theory* (John Wiley & Sons, 1991).
- ⁶⁰R. Mirman, *Group theory: An intuitive approach* (World Scientific, 1995).
- ⁶¹P. H. Butler, *Point group symmetry applications: methods and tables* (Springer Science & Business Media, 2012).
- ⁶²C. Cao, J. Hu, W. Zhang, X. Xu, D. Chen, F. Yu, J. Li, H.-S. Hu, D. Lv, and M.-H. Yung, “Progress toward larger molecular simulation on a quantum computer: Simulating a system with up to 28 qubits accelerated by point-group symmetry,” *Phys. Rev. A*. **105**, 062452 (2022).
- ⁶³K. Setia, R. Chen, J. E. Rice, A. Mezzacapo, M. Pistoia, and J. D. Whitfield, “Reducing qubit requirements for quantum simulations using molecular point group symmetries,” *J. Chem. Theory Comput.* **16**, 6091–6097 (2020).
- ⁶⁴M. Valiev, E. J. Bylaska, N. Govind, K. Kowalski, T. P. Straatsma, H. J. J. Van Dam, D. Wang, J. Nieplocha, E. Aprà, T. L. Windus, *et al.*, “Nwchem: A comprehensive and scalable open-source solution for large scale molecular simulations,” *Comput. Phys. Commun.* **181**, 1477–1489 (2010).
- ⁶⁵F. Neese, F. Wennmohs, U. Becker, and C. Riplinger, “The orca quantum chemistry program package,” *J. Chem. Phys.* **152** (2020).
- ⁶⁶M. D. Hanwell, D. E. Curtis, D. C. Lonie, T. Vandermeersch, E. Zurek, and G. R. Hutchison, “Avogadro: an advanced semantic chemical editor, visualization, and analysis platform,” *J. Cheminform.* **4**, 1–17 (2012).
- ⁶⁷A. Javadi-Abhari, M. Treinish, K. Krsulich, C. J. Wood, J. Lishman, J. Gacon, S. Martiel, P. D. Nation, L. S. Bishop, A. W. Cross, B. R. Johnson, and J. M. Gambetta, “Quantum computing with Qiskit,” (2024), arXiv:2405.08810 [quant-ph].
- ⁶⁸Q. N. developers and contributors, “Qiskit nature 0.6.0,” (2023).
- ⁶⁹Q. Sun, X. Zhang, S. Banerjee, P. Bao, M. Barbry, N. S. Blunt, N. A. Bogdanov, G. H. Booth, J. Chen, Z.-H. Cui, *et al.*, “Recent developments in the pyscf program package,” *J. Chem. Phys.* **153** (2020).
- ⁷⁰WebQC.Org, “c2v - point group symmetry character tables,” (2025), accessed: 2025-03-13.

Quantum Simulations of Chemical Reactions: Achieving Accuracy with NISQ Devices: Supporting Information

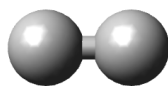
Maitreyee Sarkar¹, Lisa Roy¹, Akash Papat Gatal², Atul Kumar^{1,*} and Manikandan Paranjothy^{2†}

¹ *Quantum Information and Computation Lab, Department of Chemistry, Indian Institute of Technology Jodhpur, Rajasthan, India, 342030* and

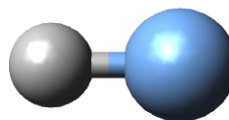
² *Chemical Dynamics Research Group, Department of Chemistry, Indian Institute of Technology Jodhpur, Rajasthan, India, 342030*

I. OPTIMIZED GEOMETRIES

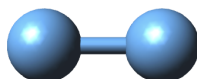
Geometry optimization values for all reactants and products, calculated using CCSD/STO-3G with NWChem, where the coordinates are expressed in Angstrom units.



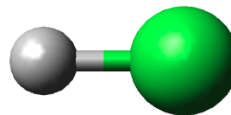
H 0.0000000 0.0000000 -0.36743273
H 0.0000000 0.0000000 0.36743273



F 0.0000000 0.0000000 -0.12163802
H 0.0000000 0.0000000 0.87299002



F 0.0000000 0.0000000 -0.69382832
F 0.0000000 0.0000000 0.69382832



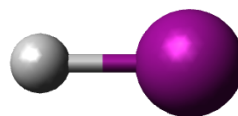
Cl 0.0000000 0.0000000 -0.09087167
H 0.0000000 0.0000000 1.25160055

* atulk@iitj.ac.in

† pmanikandan@iitj.ac.in



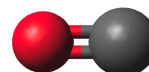
Cl 0.0000000 0.0000000 -1.06485007
Cl 0.0000000 0.0000000 1.06485007



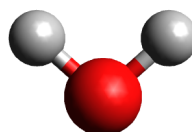
I 0.0000000 0.0000000 -0.01919551
H 0.0000000 0.0000000 1.60993328



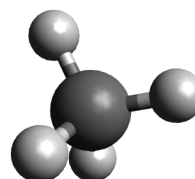
I 0.0000000 0.0000000 -1.36900912
I 0.0000000 0.0000000 1.36900912



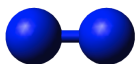
C 0.0000000 0.0000000 -0.66665088
O 0.0000000 0.0000000 0.51565030



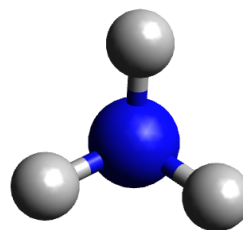
O 0.0000000 0.0000000 -0.14920525
H -0.76875446 0.0000000 0.53372741
H 0.76875446 0.0000000 0.53372741



C -0.00004309 -0.00000945 0.00002230
H 1.10818228 -0.00001016 -0.00001137
H -0.36936923 -0.78861297 0.68544214
H -0.36939931 0.98789545 0.34017445
H -0.36939931 0.98789545 0.34017445

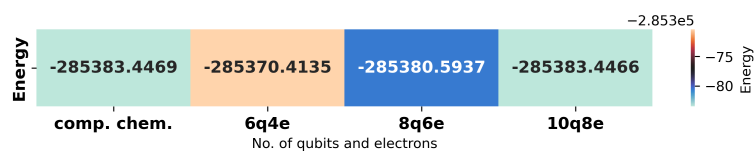


N 0.0000000 0.0000000 -0.59453116
N 0.0000000 0.0000000 0.59453116

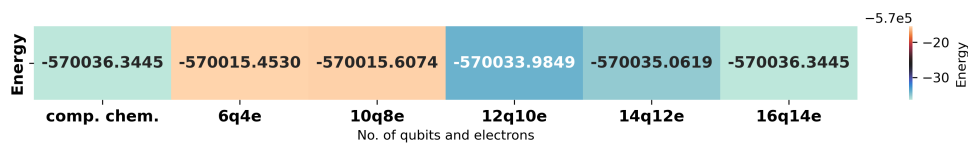


N 0.0000000 -0.0000000 -0.19630170
H -0.52537840 -0.78820401 0.30191059
H 0.94529389 -0.06088904 0.30191059
H -0.41991549 0.84909305 0.30191059

II. ENERGY VALUES FOR REACTANTS AND PRODUCTS FOR REST OF THE FOUR REACTIONS

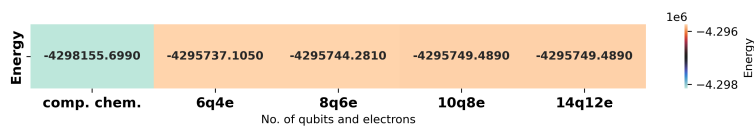


(a) Energy values for HCl Molecule

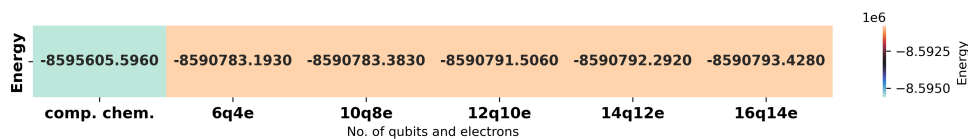


(b) Energy values for Cl₂ molecule

FIG. 7: Energy values for reactants and products of Reaction 2.

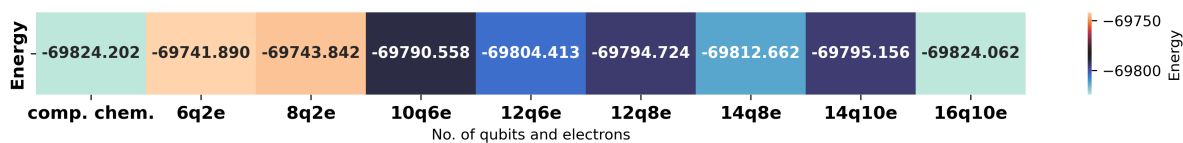


(a) Energy values for HI Molecule



(b) Energy values for I₂ molecule

FIG. 8: Energy values for reactants and products of Reaction 3.



(a) Energy values for CO Molecule

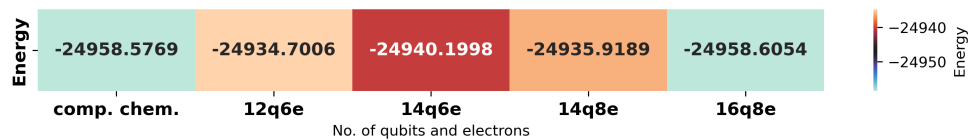
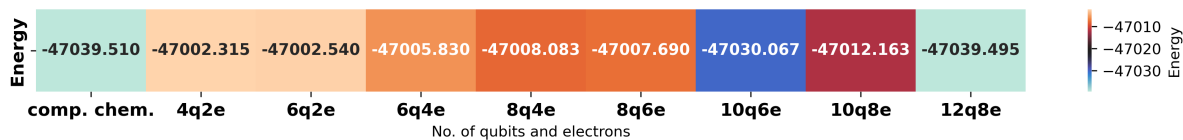
(b) Energy values for CH₄ molecule(c) Energy values for H₂O molecule

FIG. 9: Energy values for reactants and products of Reaction 4.

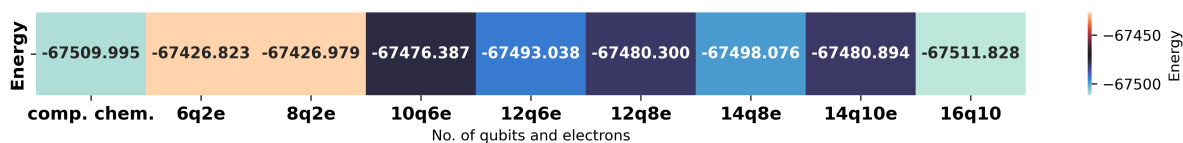
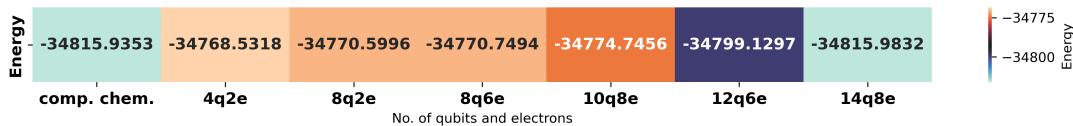
(a) Energy values for N₂ Molecule(b) Energy values for NH₃ molecule

FIG. 10: Energy values for reactants and products of Reaction 5.

III. MOLECULAR ORBITALS

Molecular orbitals for all reactants and products that contributed to the active space selection in VQE, calculated using CCSD/STO-3G with Orca.

A. Orbital Energies

TABLE I: HF

MO	No. of electrons	Orbital Energy (E_h)
0	2	-25.907079
1	2	-1.450018
2	2	-0.561731
3	2	-0.462447
4	2	-0.462447
5	0	0.552308

TABLE II: F₂

MO	No. of electrons	Orbital Energy (E_h)
0	2	-26.045178
1	2	-26.044173
2	2	-1.66929
3	2	-1.331813
4	2	-0.633172
5	2	-0.633172
6	2	-0.586152
7	2	-0.458071
8	2	-0.458071
9	0	0.421907

TABLE III: H₂O

MO	No. of electrons	Orbital Energy (E_h)
0	2	-20.244398
1	2	-1.27037
2	2	-0.614402
3	2	-0.457504
4	2	-0.392621
5	0	0.608334
6	0	0.736142

TABLE IV: CH₄

MO	No. of electrons	Orbital Energy (E_h)
0	2	-11.03007
1	2	-0.9098
2	2	-0.518757
3	2	-0.518744
4	2	-0.518727
5	0	0.715244
6	0	0.715284
7	0	0.715311
8	0	0.754338

TABLE V: CO

MO	No. of electrons	Orbital Energy (E_h)
0	2	-20.41723
1	2	-11.092398
2	2	-1.448081
3	2	-0.697329
4	2	-0.542059
5	2	-0.542059
6	2	-0.445393
7	0	0.307528
8	0	0.307528
9	0	1.015011

TABLE VI: N₂

MO	No. of electrons	Orbital Energy (E_h)
0	2	-15.512675
1	2	-15.511009
2	2	-1.42746
3	2	-0.724705
4	2	-0.562084
5	2	-0.562084
6	2	-0.535386
7	0	0.274106
8	0	0.274106
9	0	1.085938

TABLE VII: NH₃

MO	No. of electrons	Orbital Energy (E_h)
0	2	-15.306729
1	2	-1.091891
2	2	-0.571494
3	2	-0.571494
4	2	-0.354679
5	0	0.640769
6	0	0.72617
7	0	0.72617

TABLE VIII: HCl

MO	No. of electrons	Orbital Energy (E_h)
0	2	-103.722791
1	2	-10.40429
2	2	-7.849161
3	2	-7.842429
4	2	-7.842429
5	2	-1.044291
6	2	-0.565075
7	2	-0.423358
8	2	-0.423358
9	0	0.405831

TABLE IX: Cl₂

MO	No. of electrons	Orbital Energy (E_h)
0	2	-103.795634
1	2	-103.795583
2	2	-10.473339
3	2	-10.471206
4	2	-7.918623
5	2	-7.916281
6	2	-7.91029
7	2	-7.91029
8	2	-7.909448
9	2	-7.909448
10	2	-1.145444
11	2	-0.942027
12	2	-0.526112
13	2	-0.521324
14	2	-0.521324
15	2	-0.409464
16	2	-0.409464
17	0	0.116462

TABLE X: HI

MO	No. of electrons	Orbital Energy (E_h)
12	2	-23.374046
13	2	-23.374046
14	2	-6.56669
15	2	-5.178154
16	2	-5.161543
17	2	-5.161543
18	2	-1.984738
19	2	-1.97773
20	2	-1.97773
21	2	-1.96336
22	2	-1.96336
23	2	-0.730611
24	2	-0.434482
25	2	-0.293176
26	2	-0.293176
27	0	0.343146

TABLE XI: I₂

MO	No. of electrons	Orbital Energy (E_h)
24	2	-23.397506
25	2	-23.397506
26	2	-23.397506
27	2	-23.397506
28	2	-6.591794
29	2	-6.591725
30	2	-5.20538
31	2	-5.204968
32	2	-5.185372
33	2	-5.185372
34	2	-5.185338
35	2	-5.185338
36	2	-2.009892
37	2	-2.009729
38	2	-2.003544
39	2	-2.003544
40	2	-2.00346
41	2	-2.00346
42	2	-1.986513
43	2	-1.986513
44	2	-1.986511
45	2	-1.986511
46	2	-0.783959
47	2	-0.605173
48	2	-0.373232
49	2	-0.356724
50	2	-0.356724
51	2	-0.272252
52	2	-0.272252
53	0	0.132448

B. Molecular Orbitals

Molecular orbitals used for the symmetry analysis of each single and double excitation in the first reaction.

TABLE XII: MO of F₂

Atom	Orbital	MO-0	MO-1	MO-2	MO-3	MO-4	MO-5
0F	1s	0.703304	0.703833	-0.174874	0.191306	-0.000000	0.000000
0F	2s	0.016067	0.012853	0.653065	-0.766255	0.000000	-0.000000
0F	1pz	0.000000	0.000000	-0.000000	0.000000	0.684225	0.003020
0F	1px	0.002716	-0.000488	0.102207	0.082094	0.000140	-0.031610
0F	1py	0.000126	-0.000023	0.004727	0.003797	-0.003017	0.683495
1F	1s	-0.703304	0.703833	-0.174874	-0.191306	0.000000	-0.000000
1F	2s	-0.016067	0.012853	0.653065	0.766255	-0.000000	0.000000
1F	1pz	0.000000	-0.000000	0.000000	0.000000	0.684225	0.003020
1F	1px	0.002716	0.000488	-0.102207	0.082094	0.000140	-0.031610
1F	1py	0.000126	0.000023	-0.004727	0.003797	-0.003017	0.683495
Atom	Orbital	MO-6	MO-7	MO-8	MO-9		
0F	1s	-0.046464	0.000000	0.000000	0.053540		
0F	2s	0.216449	-0.000000	-0.000001	-0.267684		
0F	1pz	0.000000	-0.732441	0.000053	-0.000000		
0F	1px	-0.640713	-0.000002	-0.033835	-0.817010		
0F	1py	-0.029629	0.000053	0.731659	-0.037785		
1F	1s	-0.046464	0.000000	0.000000	-0.053540		
1F	2s	0.216449	-0.000000	-0.000001	0.267684		
1F	1pz	-0.000000	0.732441	-0.000053	-0.000000		
1F	1px	0.640713	0.000002	0.033835	-0.817010		
1F	1py	0.029629	-0.000053	-0.731659	-0.037785		

TABLE XIII: MO of HF

Atom	Orbital	MO-0	MO-1	MO-2	MO-3	MO-4	MO-05
0F	1s	-0.994789	0.252076	0.074062	-0.000000	0.000000	0.076338
0F	2s	-0.021925	-0.956314	-0.387289	0.000000	-0.000000	-0.475852
0F	1pz	-0.002412	-0.067753	0.694635	-0.000000	0.000000	-0.808593
0F	1px	0.000000	-0.000000	0.000000	0.214851	-0.976647	-0.000000
0F	1py	-0.000000	0.000000	-0.000000	-0.976647	-0.214851	-0.000000
1H	1s	0.004934	-0.142353	0.545015	-0.000000	0.000000	1.021866

IV. SYMMETRY OF EXCITATIONS

Molecule	Point Group	Group type	Abelian Subgroup Used
H ₂	$D_{\infty h}$	Non Abelian	C_{2v}
HF	$C_{\infty v}$	Non Abelian	C_{2v}
F ₂	$D_{\infty h}$	Non Abelian	C_{2v}
HCl	$C_{\infty v}$	Non Abelian	C_{2v}
Cl ₂	$D_{\infty h}$	Non Abelian	C_{2v}
HI	$C_{\infty v}$	Non Abelian	C_{2v}
I ₂	$D_{\infty h}$	Non Abelian	C_{2v}
CO	$C_{\infty v}$	Non Abelian	C_{2v}
H ₂ O	C_{2v}	Abelian	-
CH ₄	T_d	Non Abelian	C_s
N ₂	$D_{\infty h}$	Non Abelian	C_{2v}
NH ₃	C_{3v}	Non Abelian	C_s
